



Basic nutritional investigation

Lysophospholipid profile in serum and liver by high-fat diet and tumor induction in obesity-resistant BALB/c mice



Hyang Yeon Kim M.S.^a, Minhee Kim M.S.^b, Hye Min Park Ph.D.^a,
 Jiyoung Kim Ph.D.^a, Eun Ji Kim Ph.D.^c, Choong Hwan Lee Ph.D.^{a,*},
 Jung Han Yoon Park Ph.D.^{b,c,**}

^a Department of Bioscience and Biotechnology, Konkuk University, Seoul, Korea

^b Department of Food Science and Nutrition, Hallym University, Chuncheon, Korea

^c Center for Efficacy Assessment and Development of Functional Foods and Drugs, Hallym University, Chuncheon, Korea

ARTICLE INFO

Article history:

Received 5 September 2013

Accepted 8 April 2014

Keywords:

Colon cancer
 High-fat diet
 LysoPCs
 Obesity-resistant
 UPLC-Q-TOF-MS

ABSTRACT

Objective: Our previous study revealed that chronic consumption of a high-fat diet (HFD) stimulates colon cancer progression in obesity-resistant BALB/c mice. The aim of the present study was to investigate the significant alteration of metabolites caused by tumor progression and an HFD in the serum and liver in the same mouse model.

Methods: Male BALB/c mice were fed either a control diet or a HFD for 20.5 wk. The syngeneic CT26 colon carcinoma cells were injected into the right rear flank of mice after 16 wk of feeding. Metabolites in serum and liver samples were analyzed by ultra-performance liquid chromatography-quadrupole-time-of-flight-mass spectrometry-based metabolomics.

Results: HFD feeding and tumor injection induced changes in the choline-containing phospholipids, namely, phosphatidylcholines and lysophosphatidylcholines (lysoPCs), and lysophosphatidylethanolamines in the serum and liver. The majority of these metabolite changes were due to HFD feeding (11 in sera and 5 in livers) rather than tumors (3 in sera and 1 in livers).

Conclusion: The HFD- and tumor-related metabolite alterations of phospholipids, especially lysoPCs, in the liver and serum of obesity-resistant mice, suggesting that the lysoPCs are potential biomarkers for the chronic consumption of HFD in nonobese individuals.

© 2014 Elsevier Inc. All rights reserved.

Introduction

Colorectal cancer (CRC) is one of the most common cancers in the United States [1] and its incidence appears to be rising worldwide. The prognosis is directly related to the stage of the cancer at diagnosis; however, at the time of diagnosis, metastasis is already present in many patients [2]. Therefore, there is an urgent need for new prevention measures that will reduce the progression and metastasis of colon cancer. For effective

prevention of colon cancer, controlling the risk factors for cancer is important. Intake of a high-fat diet (HFD) often leads to weight gain and obesity in rodents [3] and humans [4], and is associated with a higher risk for CRC [5]. Results from epidemiologic studies indicate that overweightness and obesity are positively associated with several cancers, including colon cancer [6–8]. Although some individuals appear to be genetically predisposed to staying lean no matter what or how much they eat, others become obese. However, it is hard to determine whether the intake of an HFD indirectly affects CRC by inducing obesity or if it is an independent risk factor for this disease.

Previously, we conducted an animal study to determine whether the chronic consumption of an HFD without substantial weight gain stimulated the promotion and progression of colon cancer [9]. BALB/c mice do not become obese on an HFD [10,11]. Consumption of an HFD led to a small increase in epididymal fat pad mass and the number of fat cells in tumor tissues without any discernible weight gain in BALB/c mice injected with CT26

This work was supported by National Research Foundation of Korea grants, as funded by the Korean government (MSIP) (No. 2013R1A2A2A05004533, 2012M3A9C4048735), and a grant from the Next-Generation BioGreen 21 Program (No. PJ00952004), Rural Development Administration, Republic of Korea.

HYK, MK, and HMP contributed equally to this work.

* Corresponding author. Tel.: +82 22 049 6177; fax: +82 2 455 4291.

** Corresponding author. Tel.: +82 33 248 2134; fax: +82 33 256 0199.

E-mail addresses: chlee123@konkuk.ac.kr (C. H. Lee), jyoon@hallym.ac.kr (J. H. Yoon Park).

colon cancer cells that were derived from a spontaneously arising tumor. In those HFD-fed mice, tumor growth, as well as tumor angiogenesis and lung metastasis, was increased [9].

Recently, to better understand the biochemical mechanisms underlying obesity and the related dysfunction, metabolomic profiles of body fluids have been investigated using nuclear magnetic resonance spectroscopy or ultra-performance liquid chromatography–quadrupole–time-of-flight–mass spectrometry (UPLC–Q–TOF–MS). It has been shown that the levels of lyso-phosphatidylcholine (lysoPC) 14:0 and 18:0 were higher, but those of lysoPC 18:1 were lower in the plasma of obese men who had a high-fat intake with a lower ratio of polyunsaturated fatty acids to saturated fatty acids compared with the levels in the plasma of lean men [12]. It has been reported that metabolites such as phosphatidylcholines (PCs), lysoPCs, fatty acids, and branched amino acids were altered in the liver and plasma of obese C57BL6 mice fed an HFD [13]. HFD may induce changes in metabolites, which may subsequently influence tumor promotion and progression in obesity-resistant BALB/c mice. In the present study, using the same BALB/c mouse model, we attempted to identify the altered metabolites in the sera and livers when tumor growth and metastasis were stimulated by chronic consumption of an HFD.

Materials and methods

Animals, dietary treatment, and CT26 cell injection

Three-wk-old, male BALB/c mice were purchased from Orient Bio Inc. (Gapyung, Korea). Mice were maintained in a pathogen-free animal facility at Hallym University to acclimatize them to the laboratory conditions for 1 wk. Animals were then randomly divided into two groups and fed purified diets (Research Diets Inc., New Brunswick, NJ, USA); the HFD contained 60 kcal% fat (D12492) and the control diet (CD) contained 10 kcal% fat (D12450 B). Sixteen wk after the initiation of feeding, the two dietary groups were further subdivided into four groups: sham-injected CD (SC; $n = 15$), sham-injected HFD (SH; $n = 29$), tumor-injected CD (TC; $n = 15$), and tumor-injected HFD (TH; $n = 29$). Mouse colon carcinoma CT26 cells (5×10^4 cells) were suspended in 0.1 mL of Matrigel (BD Biosciences, San Jose, CA, USA) and subcutaneously injected into the right rear flanks of the TC and TH mice. The SH received a subcutaneous injection of 0.1 mL of Matrigel. The mice were fed continuously on the same diets. Thirty-one d after tumor cell injection, the mice were anesthetized via an intraperitoneal injection of 2.5% avertin, and blood was collected from the orbital plexus. Following blood collection, mice were sacrificed by CO₂ asphyxiation, and the livers were collected. All experimental protocols were approved by the Animal Use Committee of Hallym University (Hallym2009-123).

Histochemical analyses

Paraffin-embedded liver and adipose tissues were sectioned, deparaffinized, rehydrated, and stained with hematoxylin and eosin (H&E). For trichrome staining, a Trichrome Stain (Masson) kit (Sigma Chemical Co., St. Louis, MO, USA) was used.

Extraction of serum and liver samples

To prepare serum extracts, 150 μ L of serum was mixed with 450 μ L ice-cold methanol containing internal standards (0.5 mg/L of lidocaine and D-camphorsulfonic acid) and extracted with a mixer mill for 1 min (frequency, 30). The samples were centrifuged at 3220g for 5 min, and the supernatants were collected in Eppendorf tubes. Before UPLC–Q–TOF–MS analysis, the supernatants (160 μ L) were added to 80 μ L water.

Liver extracts were prepared according to a previously described method [14]. Briefly, liver samples (50 mg) were homogenized in 1.5 mL of ice-cold methanol/water (1:1) with a mixer mill for 2 min (frequency 30) and centrifuged at 3220g for 5 min. After centrifugation, the supernatants were collected in Eppendorf tubes and dried. Before the UPLC–Q–TOF–MS analysis, liver extract samples were resuspended in 500 μ L of methanol/water (1:1) and filtered through a 0.45- μ m polytetrafluoroethylene membrane.

UPLC–Q–TOF–MS analysis

A Waters Micromass Q–TOF Premier with UPLC Acquity system containing an Acquity UPLC BEH C18 column (100 \times 2.1 mm with a 1.7 μ m particle size; Waters, Milford, MA, USA) was performed. The mobile phase was acetonitrile and water. The initial gradient of the mobile phase was maintained at 5% acetonitrile for 1 min, after which the concentration of acetonitrile was gradually increased to 100% for 9 min. The acetonitrile was held at 100% for 1 min and gradually decreased to 0% for 2 min. Five mL of the sample was injected and the flow rate was maintained as 0.3 mL/min. Electrospray ionization (ESI)–Q–TOF–MS was performed in the negative- and positive-ion mode within a range of m/z 50 to 1000. The source temperature was set at 120°C, the nebulizer gas flow at 600 L/h, and the cone gas at 50 L/h. The capillary and sample cone voltages were set at 3000 and 40 V, respectively. Leucine enkephalin was used as the lock mass at a concentration of 0.2 mg/L and a flow rate of 0.3 μ L/min. Argon was employed as the collision gas at a flow rate of 0.3 mL/min and the collision energy was set at 50 eV.

Data processing, multivariate analysis, and other statistical analyses

UPLC–Q–TOF–MS raw data files were converted into the network common data form (netCDF, *.cdf) by Metabridge software (version 4.1, Waters Corp.). The netCDF files were automatically aligned and compared with the mass spectrometry data sets by XCMS. The resultant data matrix was processed by SIMCA-P software 12.0 (Umetrics, Umea, Sweden) and data sets were autoscaled (unit-variance scaling) and log-transformed, and then mean-centered before principal component analysis (PCA) and partial least squares discriminant analysis (PLS-DA). Univariate statistical analyses for multiple classes were performed by Student's *t* tests and one-way analysis of variance. A box-and-whisker plot was created based on the mean from data using STATISTICA (version 7.0; StatSoft Inc., Tulsa, OK, USA). Significantly different metabolites were matched to the human metabolome database (<http://www.hmdb.ca/>) and references [15] based on their retention time, accurate mass, and error (mDa).

The results for body weight, organ weight, food intake, and histological staining were expressed as the mean \pm SEM and analyzed via analysis of variance. Differences between the treatment groups were evaluated using Student's *t* test (for two groups) or Duncan's multiple range test (for four groups), using SAS for Windows version 9.2 software (SAS Institute, Cary, NC, USA). Differences were considered significant at $P < 0.05$.

Table 1
Effect of a high-fat diet and tumor injection on body weights, organ weights, and food intakes

	SC ($n = 15$)	SH ($n = 29$)	TC ($n = 15$)	TH ($n = 29$)	Diet effect (<i>P</i> -value)	Tumor effect (<i>P</i> -value)	Interaction (<i>P</i> -value)
Body weight (g)	30.3 \pm 0.4 ^c	33.8 \pm 1.2 ^a	31.6 \pm 0.3 ^{bc}	33.1 \pm 0.8 ^{ab}	0.002	0.647	0.170
Body weight–tumor weight (g)	30.3 \pm 0.4 ^b	33.8 \pm 1.2 ^a	30.4 \pm 0.3 ^b	31.1 \pm 0.6 ^b	0.008	0.049	0.041
Tumor (g)			1.26 \pm 0.18 ^b	2.04 \pm 0.26 ^a	0.037		
Liver (g)	1.74 \pm 0.05 ^b	1.87 \pm 0.11 ^{ab}	1.93 \pm 0.05 ^a	1.95 \pm 0.05 ^a	0.327	0.038	0.371
Spleen (mg)	151 \pm 10.3 ^c	170 \pm 7.81 ^c	224 \pm 10.9 ^b	307 \pm 14.3 ^a	<0.0001	<0.0001	0.014
Lung (mg)	223 \pm 11.7 ^a	220 \pm 5.52 ^a	216 \pm 2.83 ^a	219 \pm 3.84 ^a	0.861	0.483	0.618
Epididymal fat (mg)	ND	ND	242 \pm 25 ^b	446 \pm 43.8 ^a			
Energy intakes (kJ/d)	67.24 \pm 6.07 ^a	76.32 \pm 4.94 ^b	70.19 \pm 7.41 ^a	75.83 \pm 6.06 ^b	<0.0001	0.403	0.242

CD, control diet; HFD, high-fat diet; SC, sham-injected, CD; SH, sham-injected, HFD; TC, tumor-injected, CD; and TH, tumor-injected, HFD; ND, not determined. The data were evaluated using Student's *t* test (for two groups) or Duncan's multiple range test (for four groups). Means with the different letters, e.g., a, b, or c are statistically different. Differences were considered significant for $P < 0.05$.

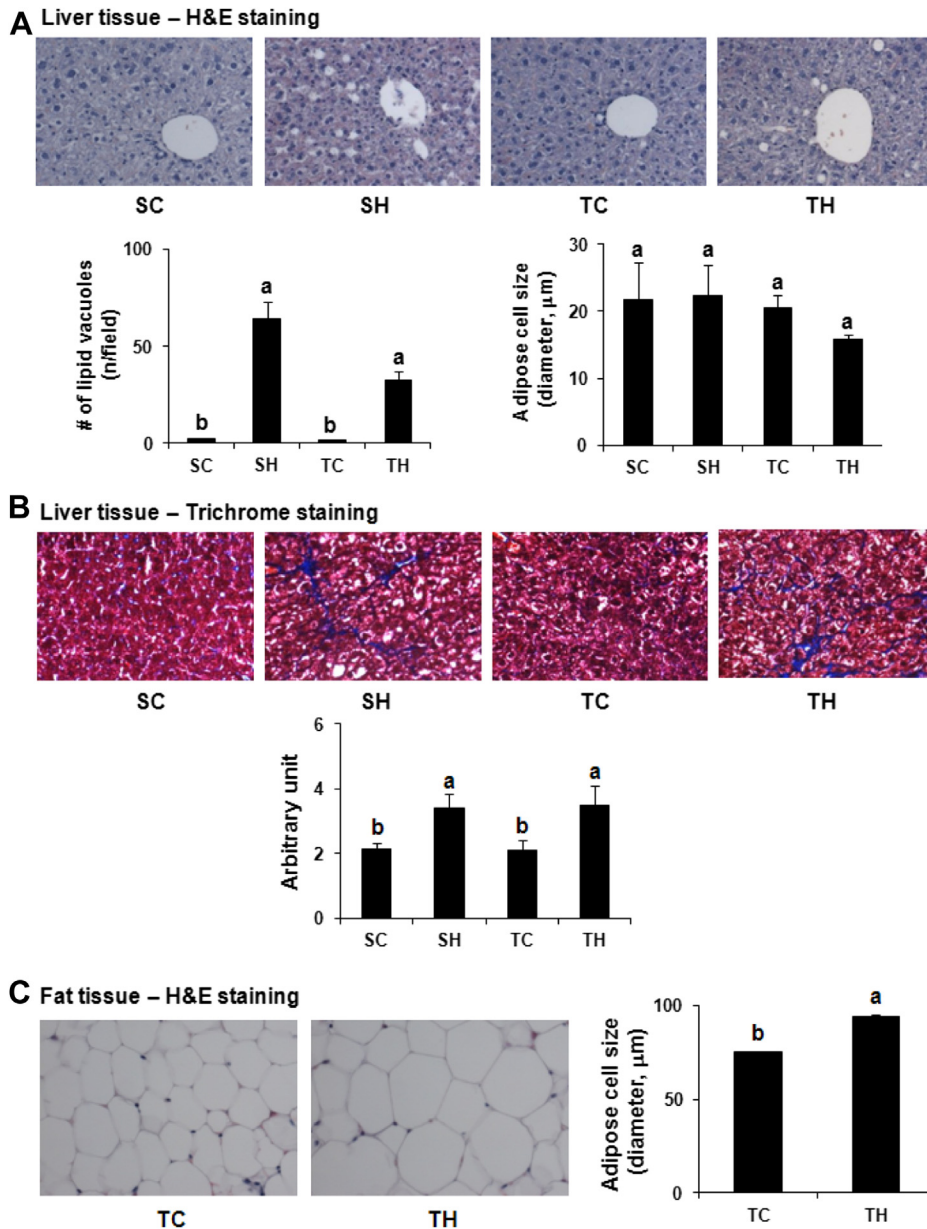


Fig. 1. Dietary fat stimulates lipid accumulation in the liver and adipose tissue in BALB/c mice. Liver sections were stained with hematoxylin and eosin (A) and trichrome (B). The sections of epididymal fat depots were stained with hematoxylin and eosin (C). SC: sham-injected, CD (n = 15); SH: sham-injected, HFD (n = 29); TC: tumor-injected, CD (n = 15); TH: tumor-injected, HFD (n = 29). The data were evaluated using Student's *t* test (for two groups) or Duncan's multiple range test (for four groups). Means with different letters, e.g., a or b are statistically different. Differences were considered significant for $P < 0.05$. CD, control diet; HFD, high-fat diet.

Results

Changes in body and organ weights in mice due to HFD feeding and/or tumor injection

At the time of sacrifice, the mean body weight was higher in the SH group than in the SC group. However, there was no difference in mean body weight and body weight (body weight–tumor weight) between the TC and TH groups. The ad libitum food intake in the SC, SH, TC, and TH groups was 4.17 ± 0.38 , 3.48 ± 0.23 , 4.36 ± 0.46 , and 3.46 ± 0.28 g/d, respectively. The food intake (g/d) was lower, whereas the energy intake (kJ/d) was significantly higher in the HFD groups than in the CD groups. Consistent with previous results [9], tumor weights were significantly higher in mice fed the HFD. Liver weights were increased in tumor-bearing mice, but the

difference between the SH and TH groups was not statistically significant. The weights of the spleens were significantly increased in tumor-bearing mice compared with the SH mice and were further increased in the TH group compared with the TC group. Lung weights did not vary among the four groups. The epididymal fat pad weights were increased in the TH mice compared with the TC mice (Table 1).

Histological changes in the liver and adipose tissue due to HFD feeding and tumor injection

H&E staining of liver sections revealed that the number of lipid vacuoles increased in the SH and TH groups. In fact, few lipid vacuoles were detected in the liver in the SC and TC groups. Trichrome staining of liver sections revealed that the intensity of

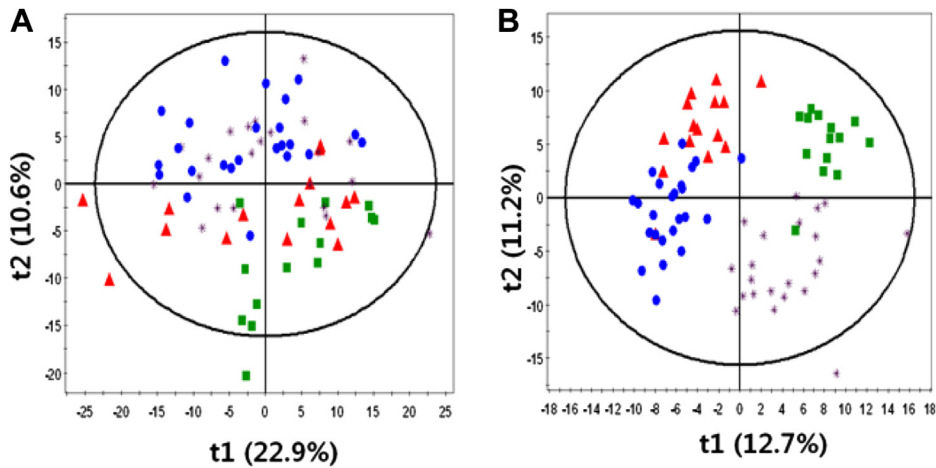


Fig. 2. PCA (A) and PLS-DA (B) score plots derived from UPLC-Q-TOF-MS data of mouse sera. \blacktriangle SC: sham-injected, CD; \blacksquare SH: sham-injected, HFD; \bullet TC: tumor-injected, CD; \ast TH: tumor-injected, HFD. CD, control diet; HFD, high-fat diet; PCA, principal component analysis; PLS-DA, partial least squares discriminant analysis; UPLC-Q-TOF-MS, ultra-performance liquid chromatography-quadrupole-time-of-flight-mass spectrometry.

the blue color (collagen contents) was also increased in the SH and TH groups compared with that in the SC and TC groups. The size of the adipocytes in epididymal fat tissue was significantly increased in the TH group relative to the TC group (Fig. 1).

Changes in metabolite profiles in mouse sera and livers due to HFD and/or tumor injection

In negative mode, 386 (in sera) and 614 (in livers) variables were used to compare the group differences resulting from the consumption of the HFD and tumor progression via PCA and PLS-DA (Figs. 2 and 3). In the serum samples, PCA and PLS-DA score plots from the first two dimensions of vector $t[1]$ explained 22.9% and 12.7% of the variation and vector $t[2]$ explained 10.6% and 11.2% of the variation among the four groups, respectively. Each group was clearly separated into four clusters in the PLS-DA score plot by diet and tumor effects. According to the diet and tumor effects, two groups were located in the opposite direction of the scores (data not shown). Arbitrary thresholds of variable

importance for the projection (VIP) > 1.0 and $P < 0.05$ were chosen to select the variables, and 99 variables were determined.

In the liver samples, PCA and PLS-DA score plots from the first two dimensions of vector $t[1]$ explained 17.4% and 15.6% of the variation and vector $t[2]$ explained 14.1% and 12.8% of the variation among the four groups. In the PLS-DA score plot, the TC group discriminated from other groups. However, each group was located in the opposite direction of the scores in the comparison with the metabolite difference between the groups by diet or tumor effects (data not shown). Among the variables, 147 were selected by VIP value (> 1.5) and P -value (< 0.05).

The discriminative metabolites in mouse sera and livers due to HFD and/or tumor injection

Sixteen serum and 8 liver peaks were annotated as significant variables with major influences on the group differences (Tables 2 and 3). The most discriminative metabolites between HFD-fed and CD-fed mice or tumor-injected and sham-injected mice in the serum included intermediates of lipid metabolism,

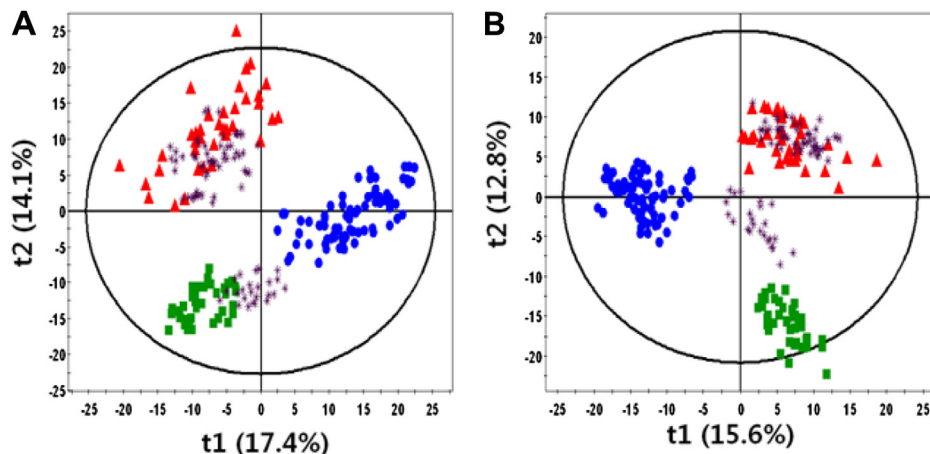


Fig. 3. PCA (A) and PLS-DA (B) score plots derived from UPLC-Q-TOF-MS data of mouse livers. \blacktriangle SC: sham-injected, CD; \blacksquare SH: sham-injected, HFD; \bullet TC: tumor-injected, CD; \ast TH: tumor-injected, HFD. CD, control diet; HFD, high-fat diet; PCA, principal component analysis; PLS-DA, partial least squares discriminant analysis; UPLC-Q-TOF-MS, ultra-performance liquid chromatography-quadrupole-time-of-flight-mass spectrometry.

Table 2

Tentative identification of significantly altered metabolites in serum of high-fat diet-fed and tumor-bearing mice by UPLC-Q-TOF-MS analysis

Group*	t _R [†] (min)	Tentative compound	Measured MS (m/z)	Molecular Formula	Error (mDa)	Adduct	
(A)	7.70	LysoPC 14:0 (1)	468.3018	C ₂₂ H ₄₆ NO ₇ P	6.7	M + H [1+]	
	8.00	LysoPC 16:1 (2)	494.3275	C ₂₄ H ₄₈ NO ₇ P	3.4	M + H [1+]	
	8.65	LysoPC 20:3 (3)	546.3572	C ₂₈ H ₅₂ NO ₇ P	1.8	M + H [1+]	
	8.72	LysoPC 16:0 (4)	496.3406	C ₂₄ H ₅₀ NO ₇ P	0.9	M + H [1+]	
	8.95	LysoPC 18:1 (5)	522.3535	C ₂₆ H ₅₂ NO ₇ P	1.9	M + H [1+]	
	8.24	LysoPC 22:6 (6)	568.3429	C ₃₀ H ₅₀ NO ₇ P	3.1	M + H [1+]	
	8.26	LysoPC 20:4 (7)	544.3428	C ₂₈ H ₅₀ NO ₇ P	3.0	M + H [1+]	
	8.29	LysoPC 18:2 (8)	520.3369	C ₂₆ H ₅₀ NO ₇ P	2.9	M + H [1+]	
	9.81	LysoPC 18:0 (9)	524.3691	C ₂₆ H ₅₄ NO ₇ P	2.0	M + H [1+]	
	9.25	LysoPE 20:0 (10)	510.3576	C ₂₅ H ₅₂ NO ₇ P	2.2	M + H [1+]	
	10.51	PE-NMe 18:1/18:1 (11)	758.5727	C ₄₂ H ₈₀ NO ₈ P	3.3	M + H [1+]	
	(B)	4.56	2-Octenoic acid (12)	187.0936	C ₈ H ₁₄ O ₂	4.0	M + FA-H [1-]
		5.09	PC 20:0/18:4 (13)	810.6039	C ₄₆ H ₈₄ NO ₈ P	3.2	M + H [1+]
6.04		PC 18:2/18:0 (14)	786.6020	C ₄₄ H ₈₄ NO ₈ P	1.3	M + H [1+]	
(C)	8.18	LysoPE 22:6 (15)	526.2936	C ₂₇ H ₄₄ NO ₇ P	0.8	M + H [1+]	
	10.45	SM d18:0/16:1 (16)	703.5732	C ₃₉ H ₇₉ N ₂ O ₆ P	1.6	M + H [1+]	

FA, formic acid; lysoPC, lysophosphatidylcholine; lysoPE, lysophosphatidylethanolamine; PE-NMe, monomethylphosphatidylethanolamine; PC, phosphatidylcholine; SM, sphingomyelin; UPLC-Q-TOF-MS, ultra-performance liquid chromatography-quadrupole-time-of-flight-mass spectrometry

Components with a *P*-value ≤ 0.05: Moderate evidence against H0

* Group affected by chronic consumption of high-fat diet (A), tumor (B), and tumor and high-fat diet (C).

† t_R, retention time.

such as lysoPCs, PCs, lysophosphatidylethanolamines (lysoPE), monomethylphosphatidylethanolamine (PE-NMe), and sphingomyelin (SM).

In the serum samples, the levels of five lysoPCs with C14:0, C16:1, C20:3, C16:0, and C18:1 were significantly decreased in the SH and TH groups, whereas the levels of four lysoPCs with C22:6, C20:4, C18:2, and C18:0, lysoPE 20:0, and PE-NMe 18:1/18:1 were increased (Fig. 4A). The levels of 2-octenoic acid, PC 20:0/18:4, and PC 18:2/18:0 were decreased in the TC and TH groups (Fig. 4B). LysoPE 22:6 and SM d18:0/16:1 were major metabolites influenced by tumors and a HFD (Fig. 4C).

In the liver samples, the levels of five lysoPCs with C22:6, C20:4, C18:2, C16:0, and C18:0 (Fig. 5A) were significantly increased in the SH and TH groups. The level of lysoPE 20:5 was higher, and that of lysoPE 18:1, and lysoPE 16:0 was lower in the SC group (Fig. 5B and C).

Discussion

Our previous study demonstrated that chronic consumption of an HFD increased tumor angiogenesis, solid tumor growth, and lung metastasis of CT26 CRC cells in obesity-resistant BALB/c mice [9]. In the present study, we investigated the changes in the levels of metabolites in the serum and liver after chronic consumption of a HFD and/or tumor injection in the same model.

HFD has been well known to be associated with obesity [16,17], diabetes [18], and inflammation [19]. Additionally, HFD-induced obesity was reported to affect lipid metabolism, including reduction of the levels of phospholipids and triglycerides in the liver [16] and increase in total cholesterol and triglyceride concentrations in the plasma [20]. We noted an accumulation of lipids in the liver and adipose tissues of the SH and TH groups (Fig. 1) even though HFD feeding slightly increased the body weight of the SH mice. The results from the trichrome staining of the liver tissues revealed that collagen contents (blue color) were increased in the SH and TH groups indicating that HFD feeding induced fibrotic changes without changes in liver weight (Table 1). Previously, we demonstrated, using the same mouse tumor models, that HFD feeding increased lipid vacuoles in the tumor tissues, as well as infiltration of macrophages into tumor and adipose tissues [9]. These results indicate that HFD feeding can induce changes in tissue and body composition, as well as inflammatory changes, without substantial alteration in tissue and body weight.

In mice fed an HFD, the number of adipose cells was increased in both liver and adipose tissues, whereas the size of adipocytes was increased only in the adipose tissues but not in the liver (Fig. 1). A previous study demonstrated that an HFD increases in the size of lipid vacuoles in the liver of obesity-prone C57BL/6N mice [21]. Current results cannot explain these differential

Table 3

Tentative identification of significantly altered metabolites in liver of high-fat diet-fed and tumor-bearing mice by UPLC-Q-TOF-MS analysis

Group*	t _R [†] (min)	Tentative compound	Measured MS (m/z)	Molecular formula	Error (mDa)	Adduct
(A)	8.23	LysoPC 22:6 (6)	612.3290	C ₃₀ H ₅₀ NO ₇ P	1.1	M + FA-H [1-]
	8.29	LysoPC 20:4 (7)	588.3295	C ₂₈ H ₅₀ NO ₇ P	0.6	M + FA-H [1-]
	8.30	LysoPC 18:2 (8)	564.3296	C ₂₆ H ₅₀ NO ₇ P	0.5	M + FA-H [1-]
	8.81	LysoPC 16:0 (4)	540.3320	C ₂₄ H ₅₀ NO ₇ P	-1.9	M + FA-H [1-]
	9.98	LysoPC 18:0 (9)	568.3624	C ₂₆ H ₅₄ NO ₇ P	-1.0	M + FA-H [1-]
(B)	7.96	LysoPE 20:5 (17)	544.2664	C ₂₅ H ₄₂ NO ₇ P	1.1	M + FA-H [1-]
(C)	8.98	LysoPE 18:1 (18)	478.2948	C ₂₃ H ₄₆ NO ₇ P	-1.5	M-H [1-]
	8.74	LysoPE 16:0 (19)	452.2782	C ₂₁ H ₄₄ NO ₇ P	-0.5	M-H [1-]

FA, formic acid; lysoPC, lysophosphatidylcholine; lysoPE, lysophosphatidylethanolamine; UPLC-Q-TOF-MS, ultra-performance liquid chromatography-quadrupole-time-of-flight-mass spectrometry

Components with a *P*-value ≤ 0.05: Moderate evidence against H0

* Group effected by chronic consumption of a high-fat diet (A), tumor (B), and tumor and high-fat diet.

† t_R, retention time.

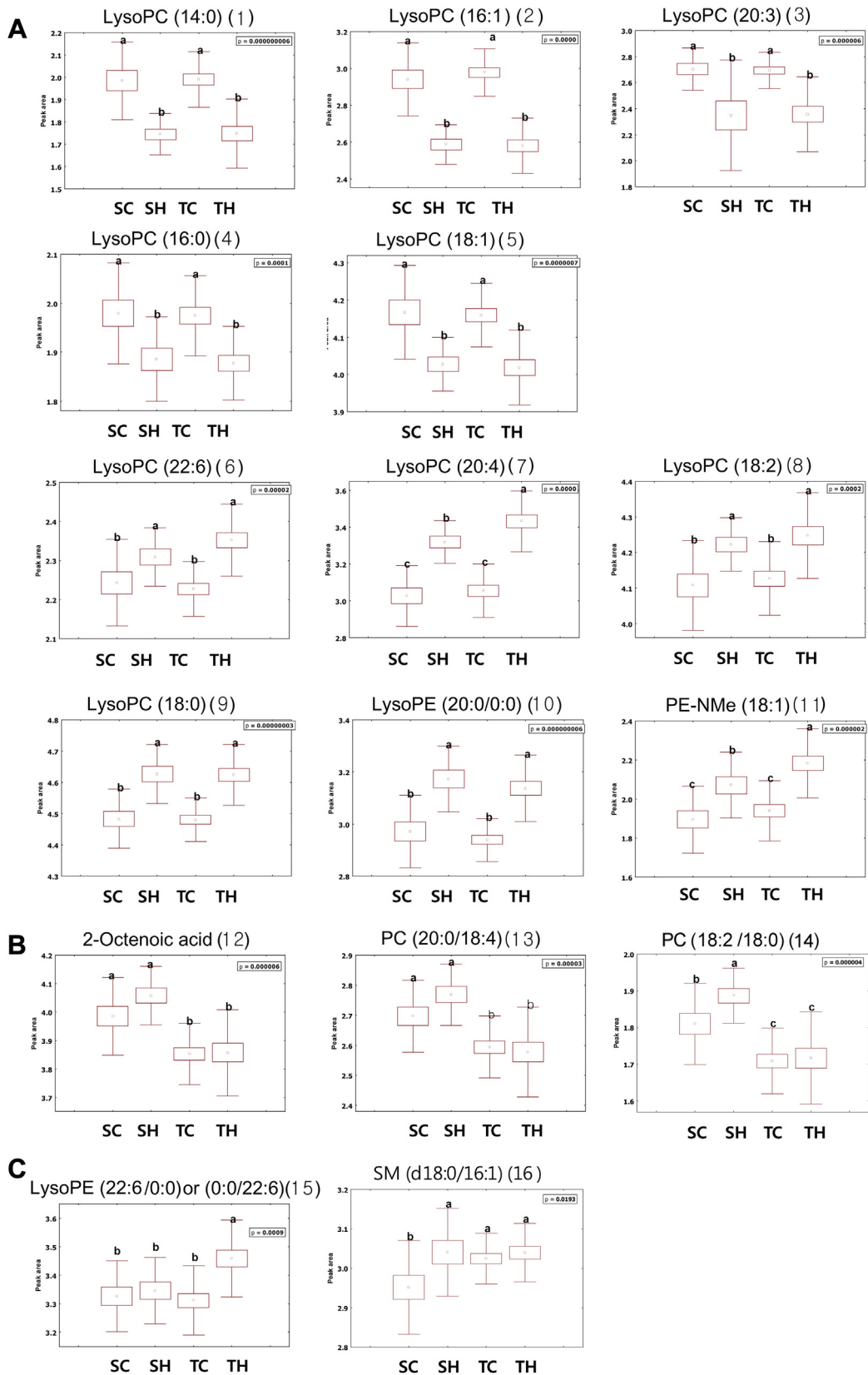


Fig. 4. Box-and-whisker plots of metabolite level changes in mouse sera. (A) Chronic consumption of a HFD, (B) Tumor, and (C) Tumor and HFD. SC: sham-injected, CD (n = 15); SH: sham-injected, HFD (n = 29); TC: tumor-injected, CD (n = 15); TH: tumor-injected, HFD (n = 29). Variables were selected by VIP value (>1.0) and P-value (<0.05). CD, control diet; HFD, high-fat diet; PCA, principal component analysis; PLS-DA, partial least squares discriminant analysis; UPLC-Q-TOF-MS, ultra-performance liquid chromatography-quadrupole-time-of-flight-mass spectrometry; VIP, variable importance for the projection.

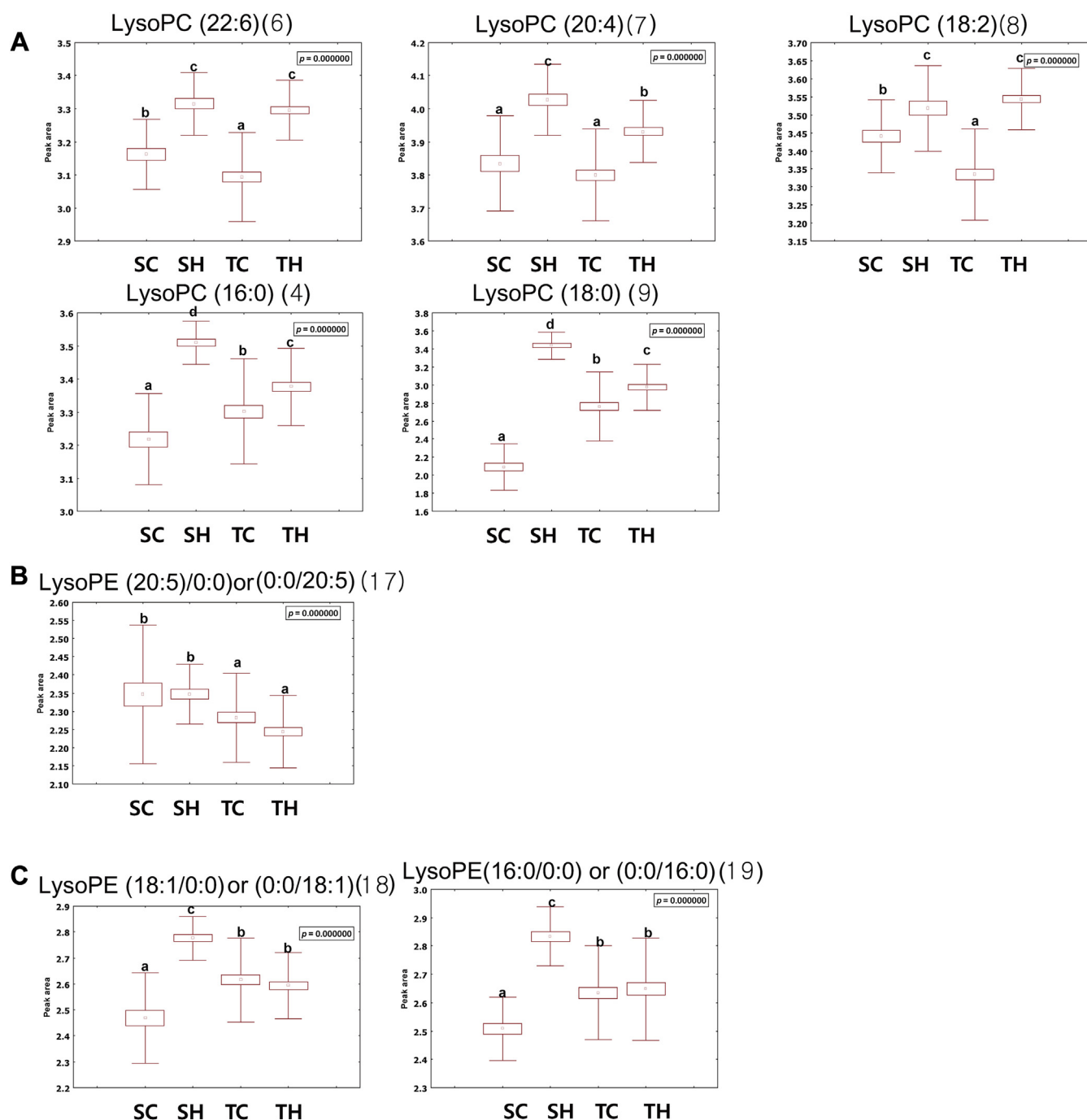


Fig. 5. Box-and-whisker plots of metabolite level changes in mouse livers. (A) Chronic consumption of a HFD, (B) Tumor, and (C) Tumor and HFD. SC: sham-injected, CD ($n = 15$); SH: sham-injected, HFD ($n = 29$); TC: tumor-injected, CD ($n = 15$); TH: tumor-injected, HFD ($n = 29$). Variables were selected by VIP value (>1.0) and P -value (<0.05). CD, control diet; HFD, high-fat diet; PCA, principal component analysis; PLS-DA, partial least squares discriminant analysis; UPLC-Q-TOF-MS, ultra-performance liquid chromatography-quadrupole-time-of-flight-mass spectrometry; VIP, variable importance for the projection.

changes in adipose cell size between the two tissues of these obesity-resistant BALB/c mice. One possible explanation is the finding that the weights of the liver did not change due to HFD feeding, whereas those of adipose tissues increased (Table 1). Because in these obesity-resistant BALB/c mice, energy intakes were only slightly increased by the HFD feeding and their body weight increases were minimal (Table 1), the majority of small extra energy was probably stored in the adipose tissues but not in the liver. Nevertheless, the extra energy increases were

probably enough to induce increases in adipose cell number in the liver.

In addition to lipid accumulation, there were changes in metabolites, primarily lipid or lipid-related, such as lysoPCs, lysoPEs, PCs, SM, and fatty acids, in the liver and serum in HFD-fed mice. LysoPCs accounted for approximately 60% of the metabolites whose levels were altered. Several studies suggested that lysoPCs generated from phospholipase A2-catalyzed hydrolysis of PC were involved in chronic inflammatory diseases,

including atherosclerosis [22], rheumatoid arthritis [23], and ischemia [24], as well as tumor progression [25,26]. It has been reported that the chemotactic ability of lysoPCs that act as chemoattractants in T lymphocytes was determined by the chain length and number of double bonds in the fatty acids of lysoPC [27]. Our results demonstrate that the chronic intake of an HFD had a stronger effect on lysoPCs than tumor injection, and variations in the levels of lysoPCs differed depending on the fatty acid composition in the serum and liver samples. Our previous results revealed that HFD feeding led to increases in the levels of various inflammatory markers, including cyclooxygenase-2 and inducible nitric oxide synthase in tumor tissues, and various cytokines/chemokines in the sera [9]. These previous results, together with the present ones, suggest that increased lysoPCs by HFD act as proinflammatory lipid mediators, thereby regulating the secretion of proinflammatory cytokines/chemokines and the expression of inflammatory enzymes. Although we noted that changes in the levels of lysoPCs and PCs were closely associated with HFD and tumor progression, future studies are needed to examine whether lysoPCs indeed regulate inflammation, as well as tumor growth and progression. It is also necessary to determine whether different lysoPCs containing various fatty acids differentially regulate these processes, because acyl distribution and composition of fatty acids within each PC are continually modified by the actions of multiple phospholipases and lyso-phosphatidylcholine acyltransferases in the PC biosynthesis pathway.

We found that the levels of four lysoPCs with C22:6, C20:4, C18:2, and C18:0 were simultaneously increased in the serum and liver of HFD-fed mice (Figs. 4 and 5). Contrary to our results, previous findings [28] showed that the levels of most lysoPCs were reduced by HFD in the plasma and liver of HFD-induced obese mice. It has also been reported that HFD caused a decrease in the levels of most lysoPCs and lysoPEs in the liver and serum in obese C57BL/6 mice, whereas the levels of PCs were increased [13]. The difference between the present results and those of other studies [13,28] suggest that metabolic responses to HFD feeding differ between obese-prone and obese-resistant animals.

Interestingly, the levels of lysoPC 16:0 decreased in the serum of HFD-fed mice, but increased in the liver (Figs. 4A and 5A). LysoPC 16:0 was the more predominant form of the lysoPCs in all analyzed samples. One study demonstrated that lysoPC 16:0 can induce growth-factor gene expression at nontoxic concentrations in cultured endothelial cells [29]. It was also demonstrated that lysoPC 16:0 exhibits very potent chemotactic properties *in vitro* [27] and induces inflammation via the production of cytokines, including interleukin (IL)-5, IL-6, and prostaglandin E₂ in ICR mice [30]. We also reported that HFD increases the serum levels of epidermal growth factor, insulin-like growth factor-I, insulin, and leptin, as well as IL-1ra, monocyte chemoattractant protein-1, interferon- γ , and stromal cell-derived factor-1 in tumor-bearing, BALB/c mice [9]. And, previous results [13] showed that the level of lysoPC 16:0 was suppressed in both serum and liver in HFD-induced obese mice. In human plasma with ovarian cancer, the level of lysoPC 16:0 depended on cancer staging [31]. Compared with various reports on change tendency of lysoPC 16:0 in plasma and serum, information concerning lysoPC 16:0 in liver is sparse, particularly in the tumor progression. So, the opposite alteration of lysoPC 16:0 level in serum and liver is not fully explained due to lack of references. Therefore, further biochemical and molecular studies on the relationship between lysoPC 16:0 and liver, as well as between lysoPC 16:0 and serum according to tumor progression is needed to evaluate and confirm the direct effects and metabolic pathway in depth.

Nevertheless, these results suggest that changes in lysoPC 16:0 may have contributed to the HFD stimulation of inflammation and lysoPC 16:0 potential as biomarkers for the chronic consumption of HFD in tumor-bearing, obesity-resistant mice.

In the serum and liver of tumor-bearing mice, the levels of 2-octenoic acid, PCs, and lysoPE, were significantly reduced compared with those in the SH mice (Figs. 4B and 5B). It has been reported that in breast and ovarian cancer cell lines, phosphocholine (PCho) levels were increased in the PC-cycle compared with normal cell lines [32]. PCho is converted to PC by cytidyltransferase, which mediates the rate-limiting step of the pathway. There may have been changes in the activity of this enzyme in the liver of tumor-bearing mice, which in turn led to a decrease in PC levels in the liver and serum. PCs are reported to induce apoptosis of cells, including colon cancer cells, vascular endothelial cells, macrophages, and adipocytes [33]. Additionally, it has been reported that the fat tissue in the phosphatidylcholine-injected rabbits showed necrosis [34]. Future studies are needed to examine the direct effect of PC on CRC cell proliferation and apoptosis.

The present results revealed that lysoPCs and PCs were the major metabolites altered in the liver and serum of HFD-fed and tumor-bearing mice and HFD played a greater role than tumors in metabolite changes. Together, these results imply that the stimulation of tumor growth and progression in HFD-fed, obesity-resistant mice may be mediated via alterations in lysoPCs. Our results clearly demonstrate that HFD induces changes in metabolite profiles, especially lysoPCs, without inducing significant changes in body or tissue weight.

Conclusion

In this study, HFD has a greater effect on metabolite changes in the serum and liver of obesity-resistant BALB/c mice. The lysoPCs possess potential as biomarkers for the chronic consumption of HFD in nonobese individuals.

References

- [1] Jemal A, Siegel R, Xu J, Ward E. Cancer statistics. *CA Cancer J Clin* 2010;60:277–300.
- [2] Hart AR, Kennedy HJ. Preventing bowel cancer: an insight for clinicians. *Ther Adv Med Oncol* 2011;3:269–77.
- [3] Lin S, Thomas TC, Storlien LH, Huang XF. Development of high fat diet-induced obesity and leptin resistance in C57BL/6j mice. *Int J Obes Relat Metab Disord* 2000;24:639–46.
- [4] Buettner R, Scholmerich J, Bollheimer LC. High-fat diets: modeling the metabolic disorders of human obesity in rodents. *Obesity (Silver Spring)* 2007;15:798–808.
- [5] Campos FG, Logullo Waitzberg AG, Kiss DR, Waitzberg DL, Habr-Gama A, Gama-Rodrigues J. Diet and colorectal cancer: current evidence for etiology and prevention. *Nutr Hosp* 2005;20:18–25.
- [6] Bianchini F, Kaaks R, Vainio H. Overweight, obesity, and cancer risk. *Lancet Oncol* 2002;3:565–74.
- [7] Calle EE, Thun MJ. Obesity and cancer. *Oncogene* 2004;23:6365–78.
- [8] Frezza EE, Wachtel MS, Chiriva-Internati M. Influence of obesity on the risk of developing colon cancer. *Gut* 2006;55:285–91.
- [9] Park H, Kim M, Kwon GT, Lim do Y, Yu R, Sung MK, et al. A high-fat diet increases angiogenesis, solid tumor growth, and lung metastasis of CT26 colon cancer cells in obesity-resistant BALB/c mice. *Mol Carcinog* 2012;51:869–80.
- [10] Olson LK, Tan Y, Zhao Y, Aupperlee MD, Haslam SZ. Pubertal exposure to high fat diet causes mouse strain-dependent alterations in mammary gland development and estrogen responsiveness. *Int J Obes (Lond)* 2010;34:1415–26.
- [11] Fearnside JF, Dumas ME, Rothwell AR, Wilder SP, Cloarec O, Toye A, et al. Phylometabonomic patterns of adaptation to high fat diet feeding in inbred mice. *PLoS One* 2008;3:e1668.
- [12] Kim JY, Park JY, Kim OY, Ham BM, Kim HJ, Kwon DY, et al. Metabolic profiling of plasma in overweight/obese and lean mice using ultra performance liquid chromatography and Q-TOF mass spectrometry (UPLC-Q-TOF MS). *J Proteome Res* 2010;9:4368–75.

- [13] Kim HJ, Kim JH, Noh S, Hur HJ, Sung MJ, Hwang JT, et al. Metabolomic analysis of livers and serum from high-fat diet induced obese mice. *J Proteome Res* 2011;10:722–31.
- [14] Masson P, Alves AC, Ebbels TM, Nicholson JK, Want EJ. Optimization and evaluation of metabolite extraction protocols for untargeted metabolic profiling of liver samples by UPLC-MS. *Anal Chem* 2010;82:7779–86.
- [15] Dong J, Cai X, Zhao L, Xue X, Zou L, Zhang X, et al. Lysophosphatidylcholine profiling of plasma: discrimination of isomers and discovery of lung cancer biomarkers. *Metabolomics* 2010;6:478–88.
- [16] Lemonnier D, Aubert R, Suquet JP, Rosselin G. Metabolism of genetically obese rates on normal or high-fat diet. *Diabetologia* 1974;10:697–701.
- [17] Galili O, Versari D, Sattler KJ, Olson ML, Mannheim D, McConnell JP, et al. Early experimental obesity is associated with coronary endothelial dysfunction and oxidative stress. *Am J Physiol Heart Circ Physiol* 2007;292:H904–11.
- [18] Winzell MS, Ahrén B. The high-fat diet-fed mouse: a model for studying mechanisms and treatment of impaired glucose tolerance and type 2 diabetes. *Diabetes* 2004;53:S215–9.
- [19] Kim SJ, Choi Y, Jun HS, Kim BM, Na HK, Surh YJ, et al. High-fat diet stimulates IL-1 type I receptor-mediated inflammatory signaling in the skeletal muscle of mice. *Mol Nutr Food Res* 2010;54:1014–20.
- [20] Libinaki R, Heffernan M, Jiang WJ, Ogru E, Ignjatovic V, Gianello R, et al. Effects of genetic and diet-induced obesity on lipid metabolism. *IUBMB Life* 1999;48:109–13.
- [21] Park S, Choi Y, Um SJ, Yoon SK, Park T. Oleuropein attenuates hepatic steatosis induced by high-fat diet in mice. *J Hepatol* 2011;54:984–93.
- [22] Schmitz G, Ruebsaamen K. Metabolism and atherogenic disease association of lysophosphatidylcholine. *Atherosclerosis* 2010;208:10–8.
- [23] Fuchs B, Schiller J, Wagner U, Häntzschel H, Arnold K. The phosphatidylcholine/lysophosphatidylcholine ratio in human plasma is an indicator of the severity of rheumatoid arthritis: investigations by ³¹P NMR and MALDI-TOF MS. *Clin Biochem* 2005;38:925–33.
- [24] Otamiri T, Sjö Dahl R, Tagesson C. Lysophosphatidylcholine potentiates the increase in mucosal permeability after small-intestinal ischaemia. *Scand J Gastroenterol* 1986;21:1131–6.
- [25] Linkous AG, Yazlovitskaya EM, Hallahan DE. Cytosolic phospholipase A2 and lysophospholipids in tumor angiogenesis. *J Natl Cancer Inst* 2010;102:1398–412.
- [26] Zhang T, Wu X, Yin M, Fan L, Zhang H, Zhao F, et al. Discrimination between malignant and benign ovarian tumors by plasma metabolomic profiling using ultra performance liquid chromatography/mass spectrometry. *Clin Chim Acta* 2012;413:861–8.
- [27] Ryborg AK, Deleuran B, Thestrup-Pedersen K, Kragballe K. Lysophosphatidylcholine: a chemoattractant to human T lymphocytes. *Arch Dermatol Res* 1994;286:462–5.
- [28] Barber MN, Risis S, Yang C, Meikle PJ, Staples M, Febbraio MA, et al. Plasma lysophosphatidylcholine levels are reduced in obesity and type 2 diabetes. *PLoS One* 2012;7:e41456.
- [29] Kume N, Gimbrone MA Jr. Lysophosphatidylcholine transcriptionally induces growth factor gene expression in cultured human endothelial cells. *J Clin Invest* 1994;93:907–11.
- [30] Hung ND, Sok DE, Kim MR. Prevention of 1-palmitoyl lysophosphatidylcholine-induced inflammation by polyunsaturated acyl lysophosphatidylcholine. *Inflamm Res* 2012;61:473–83.
- [31] Sutphen R, Xu Y, Wilbanks GD, Fiorica J, Grendys EC Jr, LaPolla JP, et al. Lysophospholipids are potential biomarkers of ovarian cancer. *Cancer Epidemiol Biomarkers Prev* 2004;13:1185–91.
- [32] Podo F, Sardanelli F, Iorio E, Canese R, Carpinelli G, Fausto A, et al. Abnormal choline phospholipid metabolism in breast and ovary cancer: molecular bases for noninvasive imaging approaches. *Curr Med Imaging Rev* 2007;3:123–37.
- [33] Li H, Lee JH, Kim SY, Yun HY, Baek KJ, Kwon NS, et al. Phosphatidylcholine induces apoptosis of 3T3-L1 adipocytes. *J Biomed Sci* 2011;18:91.
- [34] Rittes PG, Rittes JC, Carriel Amary MF. Injection of phosphatidylcholine in fat tissue: experimental study of local action in rabbits. *Aesthetic Plast Surg* 2006;30:474–8.